Poly(lactic acid): flow-induced crystallization

Alicyn Rhoades[1] and Roberto Pantani[2]

[1]Department of Plastics Engineering, Penn State Erie, the Behrend College. Erie, PA 16563 – United States, email: alicyn@psu.edu

[2]Department of Industrial Engineering, University of Salerno, via Giovanni Paolo II, I-84084, Fisciano (SA) – Italy, email: rpantani@unisa.it

Abstract

Poly(Lactic Acid) is surely one of the most interesting commercially available biodegradable polymers. Being a slowly-crystallizing material, it generally does not have the time to crystallize at the cooling rates involved in the common processing techniques. However, the properties induced by crystallinity are extremely interesting for tuning the characteristics of the obtained parts, and this leads the research to find the routes to an enhancement of PLA crystallization kinetics. During processing, polymer melts are subjected to very high deformation rates, and the stretch resulting from this orientation gives rise to shorter crystallization times and also to peculiar crystalline structures. The so-called flow-induced crystallization is therefore a phenomenon that for PLA can be considered strategic toward the realization of parts with enhanced properties. In this work, a state of the art on flow-induced crystallization of PLA is presented.

Contents

Nomenclature

E	Tensile modulus
ΔG_f	Energy barrier for flow induced crystallization
ΔG_q	Quiescent nucleation energy barrier
ΔS_f	Degree of entropy reduction by shear
G	Growth rate
k_a	Avrami kinetic constant
N	Nucleation density
n_a	Avrami exponent
$t_{1/2}$	Half crystallization time
X	Absolute crystallinity degree
$\dot{\gamma}$	Shear rate
ε	Ultimate strain
ξ	Relative crystallinity degree
ϱ	Density
σ	Tensile strength

Introduction

Poly (lactic acid) (PLA) is presently the most successful commercial bio-based thermoplastic, boasting applications that range from food packaging to medical implants. PLA is also the most commonly used polymer in fused filament modeling style of additive manufacturing. PLA is both *bio-renewable*, meaning the raw materials used to produce the polymer are from non-petroleum (plant) sources and *bio-degradable*, meaning the polymer will decompose relatively quickly into lactic acid when subject to heat, moisture and basic conditions. The mechanical and degradation properties of PLA are direct functions of the polymer microstructure. Microstructure, in turn, is a function of the polymer backbone chemistry (isomer content and chain branching) as well as molecular weight and molecular weight distribution. However, polymer microstructure is also strongly influenced by the melt flow incurred during polymer processing. Developing ideal mechanical and degradation property profiles in a manufactured part therefore require a comprehensive understanding of PLA chemistry and melt crystallization kinetics under flow, much of which is still under development in the research community. For example, the idealized PLA microstructure to optimize mechanical tensile strength (oriented crystal microstructure) is obviously different than that which would result in the toughest PLA sample (semi-crystalline content with idealized free volume), but the current state of the art cannot yet dial in conditions to produce such microstructure with a high level of certainty. Neither are the processing methods broadly optimized to control microstructure due to the competing degradation and the slow crystallization processes of PLA. Nonetheless, rapid progress is being made on many fronts. This chapter aims to provide the reader with a summary the current understanding of flow induced crystallization (FIC) as it is observed and quantified for PLA, and also review the polymer processing techniques that potentially induce FIC in PLA.

Generalities on PLA crystallization

Lactic acid has an asymmetric carbon atom, which leads to two optically different active forms, L-lactic acid and D-lactic acid. The polymers coming from pure L- or pure D- forms are referred to as PLLA and PDLA, respectively. Commercially, the homopolymer in L-form, or L-form-rich copolymers are the most important. The abbreviation PLLA is commonly adopted also for L-form-rich copolymers. This review focuses on PLLA, which is a crystallizable polymer with a maximum crystallinity of 60–70% in the case of the homopolymer [1]. The quiescent crystallization kinetics of PLLA is slow, with half times of the order of minutes [2]. PLLA is polymorphic: under quiescent conditions, when crystallized above 120°C, the material presents the *α-phase* whereas the *α'-phase* develops at temperatures lower than about 100°C [3]. Both phases can develop between 100 and 120°C. The α'-crystals are less ordered, stable at the temperatures at which they form, but able to transform into the more stable α-crystals upon heating at about 150°C. Other crystalline phases are found in PLLA: the β-form, which develops when the α-phase is stretched at elevated temperatures [4], and the γ-form, which is generated by epitaxial crystallization [5].PLLA and PDLA can co-crystallize together and form a stereocomplex which presents a melting point about 50°C higher than that of PLLA homocrystal.

PLLA is a slowly crystallizing polymer, with the fastest crystallization rate at about 110°C [1, 6, 7]. The crystallization half time increases on increasing the molecular weight and the D-Lactide content. For the homopolymer, molecular weights of about 100KDa allow a maximum crystallization half time of the order of one minute. Commercial PLLA grades, with D-Lactide contents of about 2%, have crystallization times about one order of magnitude larger [8] [9]. This slow crystallization kinetics make the material unable to crystallize at the cooling rates involved in normal processing conditions. However, significant crystal microstructure is sometimes found in injection molded parts [10], thus suggesting that flow can significantly influence the phenomenon of crystallization, as better explained below in this chapter.

The overall crystallization kinetics of PLA is composed of two independent phenomena: crystal nucleation and subsequent crystal growth.

Quiescent Growth rate

In quiescent, isothermal conditions, PLA crystalline structures grow spherically with a constant growth rate, G. This is confirmed when the evolution of crystallinity under quiescent conditions is analyzed by Avrami's model

$$\xi(T, t) = 1 - exp[-(k_a(T)\, t)^{n_a}] \qquad (1)$$

In which ξ is the relative crystallinity degree, k_a is the Avrami costant and n_a is the Avrami exponent, this latter takes a value close to 3 (describing predetermined, spherical growth) independently on the molecular weight and on the D-Lactide content [2, 11].

The direct measurements of growth rate by polarized optical microscopy (POM) reveal that this phenomenon depends on the molecular weight and on the D-Lactide content [1]. In particular, a higher content of D-lactide and a higher molar mass decrease the spherulitic growth rate [7].

The maximum growth rate for PLLA spherulites is reported as about 30 micron/min [12] at 110-120°C. In this range of temperatures, the maximum growth rate is normally found for most of PLLA grades. Commercial grades present a maximum growth rate of about 2.5 micron/min in the range 105-130°C [2, 6]. Just for comparison, in the same range of temperature isotactic polypropylene presents a growth rate of about 1 μm/s, or about two orders of magnitude larger.

Quiescent nucleation

If overall crystallization rate and growth rate are measured and reported in many literature works, the data concerning the nucleation rate of PLA are rare. It is generally assumed that the nucleation phenomenon in commercial PLA grades is athermal (heterogeneous), so

that a given number of nuclei are formed at each temperature instantaneously, and the number does not change with time. Sporadic nucleation, with a number of nuclei increasing with time, has been found at temperatures below the glass transition [3].

In most of literature works, the number of nuclei per unit volume (nucleation density, N) in isothermal conditions is estimated by using the relationship between volume space filling and crystallization half time, $t_{1/2}$:

$$t_{1/2} = \frac{\ln(2)}{\left(\frac{4}{3}\pi N G^3\right)^{\frac{1}{3}}} \qquad (2)$$

which allows calculating the nucleation density N from the Growth rate and the crystallization half time assessed by means of calorimetric data:

$$N = \frac{3}{4\pi}\left(\frac{\ln(2)}{G\, t_{1/2}}\right)^3 \qquad (3)$$

It has to be mentioned that the presence of a third power makes the calculation of N extremely sensitive to uncertainties in the measurements of G and $t_{1/2}$.

On the other hand, measuring N from POM is difficult because the nuclei can be counted on a surface, but the observed volume is not easily evaluated. This is the reason why many data of nucleation density are expressed in nuclei/mm² (namely surface nucleation density) [6], which is useful for understanding a trend, but not for having data of volume nucleation.

Just a few literature works report the volume nucleation density. Some results are summarized in Figure 1. It can be noticed that, apart from the huge scattering of data (notably also measurements made on the same PLA grade provide differences of about two orders of magnitude), the nucleation rate of PLA is comparable to that of iPP. This means that the enormous difference in overall crystallization rate between the two polymers can be ascribed mainly to the growth rate, which moreover appears in the equation for half-time of crystallization (eq. 2) with a power 3.
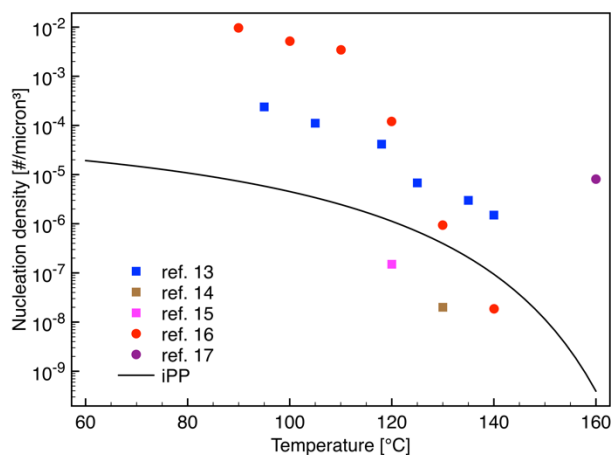
Figure 1 Nucleation density of PLA grades from literature works. Squares refer to the same PLA grade (2002D from Natureworks) [13–15]. Circle refer to a PLA with D-content of 1.1-1.7%[16, 17]. The line refers to the nucleation density measured on a iPP [18] and is given for comparison.

Stereocomplex crystallization

Typically, PLA is produced via the ring-opening polymerization of lactide, which is the cyclic dimer of the chiral lactic acid. As such, there are three diastereoisomers of lactide; L-lactide (composed of two L-units, D-lactide (composed of two D units), and meso-lactide (containing one of each D and L unit). Depending on the ratio of these diastereoisomers in the monomer feed, polymerized PLA can be of several stereostructures, including poly(L-lactide) (PLLA), poly(D-lactide) (PDLA), poly(DL-lactide)(PDLLA) and other stereocopolymers. D- and L-isomers of PLA in helical conformations can interact side by side with each other to create a specific crystalline chain-packing state that is called "stereocomplex" (SC) [19]. SC content within PLA has a strong effect on crystallization from the melt. In particular, the overall crystallization rate of the stereocomplex is higher with respect to crystallization of PLLA homocrystal (HC). It is recognized that this increase of crystallization rate is primarily due to stereocomplex crystallites that act as nucleating agents for PLLA spherulites [20], but there is also a slight increase of growth rate (within

20%) observed only at low percentages of stereocomplex [21]. The nucleating effect is considerable: it is reported that a 30-fold reduction on the crystallization half time can be reached by using 10% by weight of low-molecular weight in PDLA, whereas the same amount of talc in the same material only allowed a reduction by a factor of about two [22]. The results reported in the literature make the SC extremely interesting for enhancing the crystallization rate [23].

While the lamellar PLLA crystallites exhibit a hexagonal form, the SC crystal display a triangular morphology as observed with transmission electron microscopy or atomic force microscopy. Additionally, the wide angle x-ray diffraction (WAXD) pattern of SC-PLA differs from the diffraction pattern of PLLA; the WAXD pattern comparison is shown in Figure 2 [24, 25].
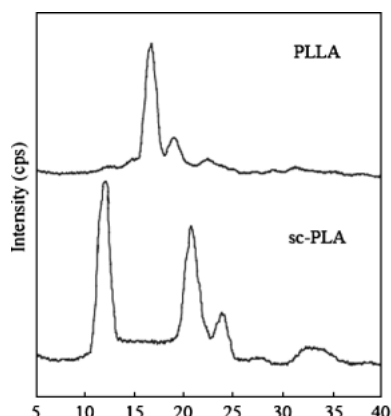

Figure 2. Wide Angle X-Ray Diffraction pattern for PLLA and SC-PLA, indicative of different crystal structures formed upon cooling from the melt. [24] Copyright 2006, John Wiley and Sons.

Perhaps as a result of the enhanced and different crystallization, SC-PLA also boasts improved thermal resistance, hydrolytic stability, and mechanical properties relative to PLLA [26, 27].

Table 1 – Summary physical and mechanical properties of PLA, PLLA, and PDLLA [27]

Properties		PLA	PLLA	PDLLA
Density (ϱ)	g/cm³	1.21 - 1.25	1.24 – 1.30	1.25-1.27
Tensile strength (σ)	MPa	21 - 60	15.5 - 150	27.6 - 50
Tensile modulus (E)	GPa	0.35 - 3.5	2.7 - 4.14	1 - 3.45
Ultimate strain (ε)	%	2.5 - 6	3.0 – 10.0	2.0 – 10.0
T_g	°C	45 – 60	55 – 65	50 – 60
T_m	°C	150 – 162	170 – 200	amorphous

Generalities on Flow Induced Crystallization

While the quiescent crystallization of PLA has been broadly studied, the achieved understanding is not directly transferred to the polymer engineering of PLA, because quiescent crystallization studies describe PLA behavior in the absence of melt flow and orientation. For practical engineering implementation, the flow-induced crystallization (FIC) of PLA must also be understood.

Flow induced crystallization is a broad term that describes the crystallization of polymers during and after they have been subject to shear flow [28]. Historically, most experimental investigations of FIC have focused on olefin-based polymers, and models which describe FIC behavior are almost exclusively derived from these flexible polymers. Research specific to FIC in PLA provide important insight to the influence of the flexible backbone, intramolecular interactions, and SC aspects of PLA.

Relative to quiescent crystallization, FIC exhibits increased nucleation density, the crystallization kinetics are accelerated, and the resulting microstructure is oriented or anisotropic. To explain the thermodynamics which drive FIC phenomena the entropy-reduction model (ERM), originally proposed by Flory, is perhaps the most widely-accepted model [29–31]. During melt flow, some fraction of the longest

chains become oriented and stretch in the melt. This orientation leads to an entropy reduction, which lowers the energy barrier for FIC according to equation 4. The energy barrier for FIC is expressed in terms of the quiescent nucleation energy barrier (ΔG_q) and the degree of entropy reduction by shear (ΔS_f) [32];

$$\Delta G_f = \Delta G_q + T_s \Delta S_f \quad (\Delta S_f < 0) \qquad (4)$$

Both the reptation time and the Rouse time of the polymer are important characteristics that dictate the amount of flow required to induce FIC [33]. Three resulting microstructure regimes have been identified that stem from the competition of shear flow and polymer relaxation in the FIC process. The first regime occurs if the shear rate does not exceed the reciprocal of the relaxation time, no noticeable FIC effects will be observed. The second regime requires increasing the strength of the shear flow such that the shear rate exceeds the reciprocal of the relaxation time but does not exceed the reciprocal of the polymer Rouse time. This regime will yield enhanced point-like nuclei and accelerated crystallization kinetics, but the morphology will remain isotropic. The third regime, which results from increasing shear work, will result in oriented or "row" nuclei. If the shear rate exceeds the reciprocal of the polymer Rouse time then these long chains extend during flow, and ultimately form the anisotropic shish-kebab structures indicative of the fourth regime [34]. While many outstanding questions remain with regard to the exact mechanism of nucleation in FIC, most studies indicate that the extended chains act as precursors to nucleate crystallization.

As the reader will observe, to date no published studies have shown all *four* regimes for PLA in a single study that quantifies the shear work required to induce enhanced nucleation (second regime), oriented nuclei (third regime) and shish-kebab structures (fourth regime). However, taking a comprehensive look at the literature, one can hypothesize that PLA behaves according to the three-regime model when comparing the results of different researchers in light of their experimental protocol. For example, pooling the data from Zhong and coworkers [35] with that of Xu and coworkers [36], the following data indicate that increasing shear work in PLLA (Natureworks 4032D) prior to crystallization at 135 °C can yield each of the four regimes. In other words, increasingly

intense shearing conditions must be introduced to cause the PLA melt to crystallize in increasingly nucleated and oriented microstructure. These two studies will be discussed in more detail later in the text.

Table 2. Summary conditions used to produce FIC effects per regime I (no effect), regime II (enhanced nucleation), regime III (oriented nuclei) and regime IV (shish kebab) in PLLA (Natureworks 4032D) [35, 36]

	T_m (°C)	T_c (°C)	Sample thickness (µm)	Shear time (s)	$\dot{\gamma}$ (s⁻¹) I → II	$\dot{\gamma}$ (s⁻¹) II → III	$\dot{\gamma}$ (s⁻¹) III → IV
Zhong	190	135	10	variable	0.0076	0.45	
Xu	200	135	20	1			100

Methods for Assessing

The characterization techniques used to assess the extent of FIC that a polymer undergoes after shear flow are much the same as those used to characterize quiescent crystallization [37]. POM is used to identify both enhanced nucleation density and anisotropy of the final microstructure. Accelerated crystallization kinetics can be observed using hot stage microscopy, where the appearance of crystal growth occurs faster than the quiescent equivalent upon cooling or isothermal crystallization. Rotational rheology is commonly used to first impose a controlled shear field on the melt and then subsequently observe crystallization through a very small oscillatory motion at constant temperature or during cooling. [34, 38, 39] Calorimetry will reveal higher crystallization temperatures upon cooling of sheared samples, and the stable flow-induced nuclei are known to nucleate crystallization at high supercooling via fast scanning calorimetric measurements [40–42]. In addition, both small and wide angle X-Ray diffraction techniques are used to quantify the crystalline fraction content, orientation, and phase characteristics.

Flow-Induced Crystallization of PLA

Both renewable sourcing and controlled biodegradation make PLA a top candidate for emerging engineering applications of the future. However, to optimize mechanical properties and degradation profiles, the crystallization of PLA must be manipulated by engineers in order to control PLA microstructure during polymer product manufacturing. Most manufacturing processes used to transform PLA into the melt such as molding, casting, and extrusion subject molten PLA to a shear flow. Consequently, the flow-induced crystallization of PLA emerges as a critical phase transformation that is generating much interest from industrial and academic researchers alike [43]. Like other high polymers, PLA is known to form spherulitic morphology after zero or low shear deformation, to experience enhanced nucleation and isotropic growth at after experiencing moderate flow, and to exhibit cylindrites and shish kebab structures after strong shearing in the melt. Examples of PLA spherulites and shish kebabs are shown in Figure 3. The specific relationships between molecular architecture, molecular weight, shearing temperature, shear rate, and crystallization temperature that ultimately drive the resulting morphology are not thoroughly understood at present. However, much progress towards quantifying the FIC behavior of PLA has taken place in recent years, forming the foundation of current active research in PLA flow-induced crystallization.
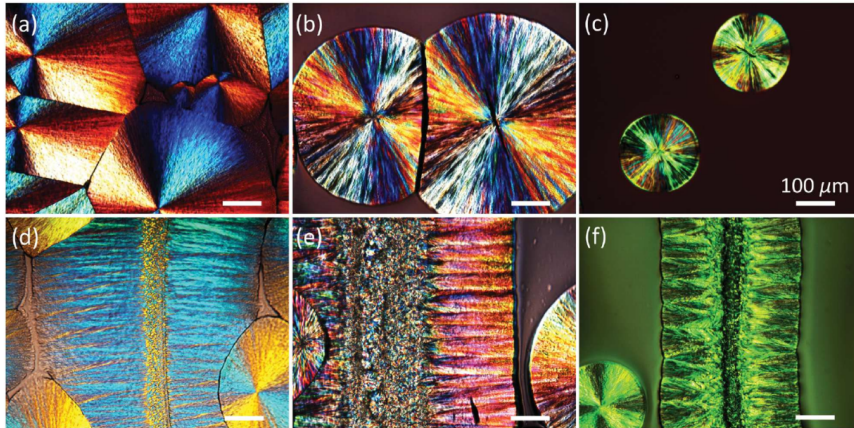
Figure 3. POM Imaging reveal PLA sphereulites (a-c) and cylindries or shish-kebabs (d-f) formed at 150 °C (a,d) 165 °C (b,e) and 180 °C (c,f). From [44]. Copyright 2016, John Wiley and Sons.

The first forays into the FIC behavior of PLA were broached by those interested in the solidification of PLA fibers [45–48]. The extreme deformation experienced by the polymer during fiber formation results in both typical FIC where the polymer is first oriented and then allowed to crystallize, in addition to the deformation that occurs when the original crystal structure is disrupted by solid-state drawing [49]. The PLA fibers studied by Cicero and coworkers displayed increased melting temperature and greatly improved mechanical properties relative to the quiescently crystallized PLA. Similarly, Mahendrasingam found that shish kebab morphology developed in PLA after rapid tensile deformation [50].

Effect of FIC on nucleation rate

With respect to FIC forming upon melt cooling, Fitz and coworkers were the first to explore the influence of shear flow on the isothermal crystallization kinetics of PLLA [51]. After a controlled shear step at crystallization temperatures between 80 °C and 150 °C (shear rate 1 s^{-1}, duration 1 second, sample thickness 300 μm and diameter 30 mm) they observed increase in nucleation density and an increase in the rate of

conversion, relative to the quiescent equivalent. Polarized light microscopy is commonly used to observe the increased nucleation density that results from a previous shear step. Such images were developed by Zhong and coworkers as they determined the critical shear rates to increase the nucleation rate of PLA, and are shown in Figure 4.
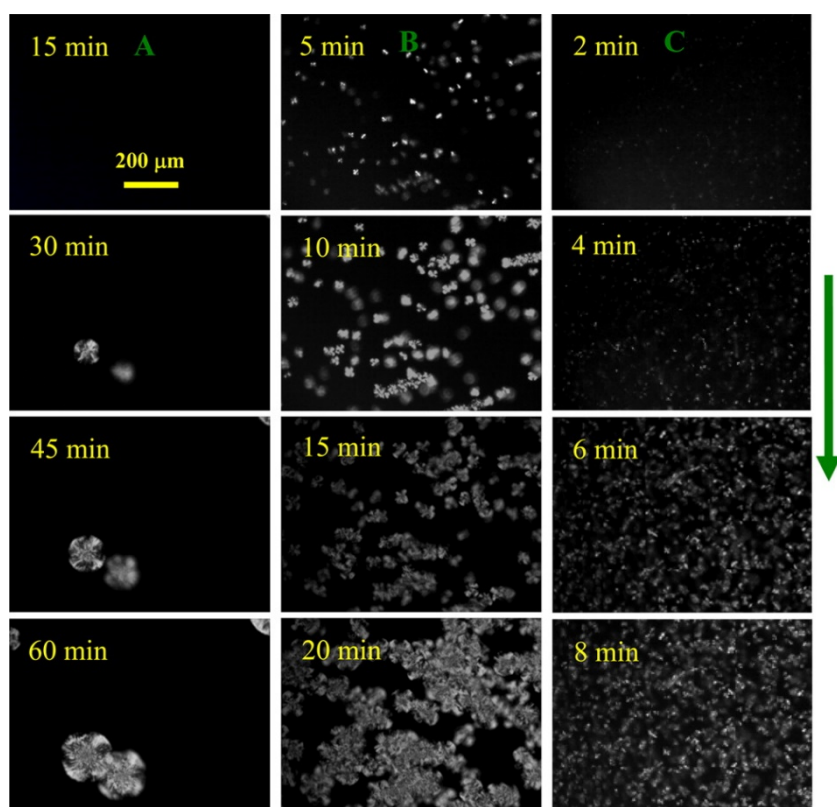

Figure 4. Selected POM micrographs for PLA during isothermal crystallization at Tc of 135 °C after being sheared at a shear rate of 10 s⁻¹ for different times of (A) 0 s, (B) 4 s, and (C) 40 s. The yellow color scale bar in the top left micrograph represents 200 μm and is applied to all other micrographs. Crystallization times are indicated in the micrographs. The green color arrow on the right side of the figure indicates the shear flow direction. From [35], Copyright 2013, American Chemical Society.

In this study, the shear rate and time requirements necessary to enhance the nucleation of PLA (2% D content, 160 kg/mol), a rotational rheometer was used. The critical shear rates for the orientation and stretch of the longest chains at 135 °C were determined to be 0.0076 and

0.45 s^{-1}, respectively. The samples detailed in Figure 4 were subject to a shear rate of 10 s^{-1} for the indicated duration, clearly exceeding the threshold of 0.45 s^{-1}. After shear for the indicated time, the nucleation rate of the PLA increased with increasing shear time. Using similar rheological techniques, Fang and coworkers observed the onset of crystallization of PLA (4% D content, 87 kg/mol) after the polymer was held in the melt at 250 °C before being cooled to the target shearing temperature of 120 °C where a steady shear pulse was applied for the indicated time. After shearing, an oscillatory time sweep was used to monitor the increase of storage modulus (G') with time. The storage modulus increases as crystallization occurs in the melt, and is directly related to the relative crystallinity by applying a logarithmic normalization of the G' data as was developed by Pogodina and coworkers [52]. Without shear, the onset of increasing storage modulus due to the onset of crystallization, t_0, is approximately 7300 seconds. Considering the sheared samples, it can be easily seen that the onset of crystallization detailed in Figure 5 decreases with increasing shearing time.
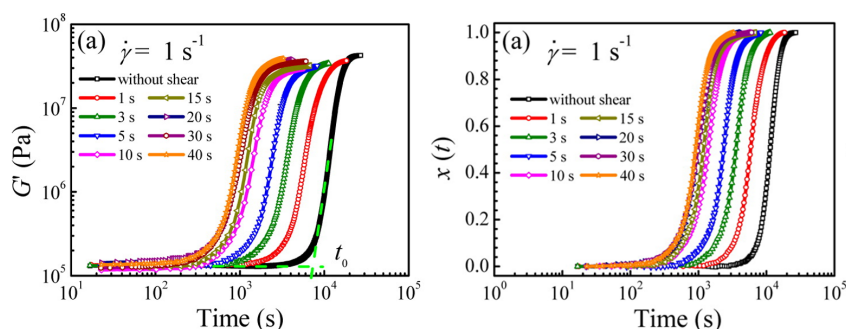
Figure 5. Changes of storage modulus, G', and percent crystallinity, x(t), with time during crystallization at Tc of 120 °C at the shear rate of $\dot{\gamma}$ = 1 s–1 with different shear time for linear PLA (4% D content, 87 kg/mol). [15] Copyright 2013, American Chemical Society.

The half-times of crystallization for the sheared and quiescent PLLA samples are shown in Figure 6. Notice that the accelerating influence of FIC is most dramatic at high crystallization temperatures. At these high temperatures, crystallization is controlled by heterogeneous nucleation, and the order introduced to the melt during flow yields precursors that act to nucleate the surrounding melt [53].

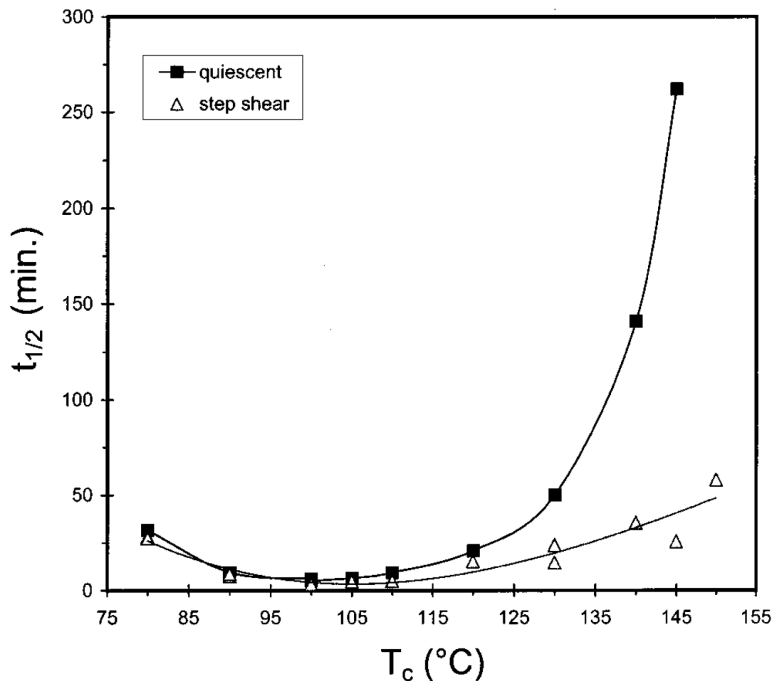**Figure 6.** Crystallization half-time as a function of crystallization temperature for quiescent and sheared PLLA samples. [51] Copyright 2002, American Chemical Society.

Using shear rates less than or equal to 5 s^{-1}, Fitz et al. did not observe anisotropic or fibrillary morphology in PLLA (M_n and PDI were 50,000 g/mol and 2.34, respectively). However, to reach anisotropic morphologies, a stronger dose of deformation must be applied to the melt. Stronger shear fields were subsequently explored, revealing the relationship between shear flow, crystallization kinetics and resulting morphology. Huang and coworkers used an optical shear cell to first induce flow in PLLA (M_n and PDI were 34,100 g/mol and 1.39, respectively) and then directly observed the isothermal crystallization at several temperatures after shearing. They determined that applying a shear rate of 20 s^{-1} for five seconds was required to induce a complete conversion to α-crystal content morphology after isothermal crystallization at 115 °C. However, all shear rates studied caused an increase in α-crystal content relative to unsheared samples for a given crystallization temperature [54]. Additionally, in sheared PLLA the α-crystal was able to form at lower temperatures than in the quiescent

17

samples. For example, after crystallization at 96.5 °C the α-crystal is typically a minor component amongst the majority α'-crystal mesophase. As shown in Figure 7, with increasing shear the WAXD reflections (0 1 0) (2 1 0) and other reflections at higher 2θ become stronger with increasing shear rate, indicating more ordered α-crystal content.
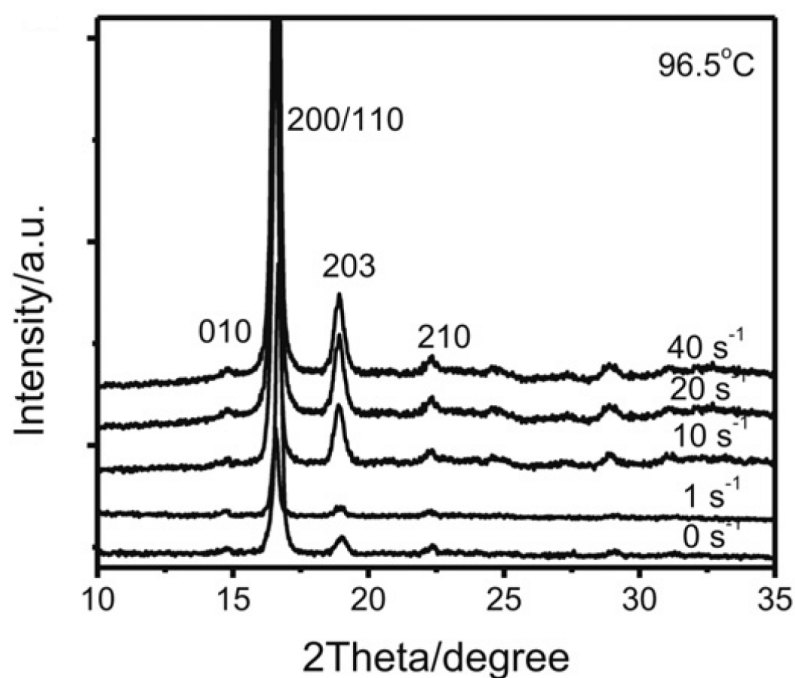
Figure 7 WAXD Patterns of PLLA crystallized at 96.5 °C after being subject to different shear rates. [41] Copyright 2001, American Chemical Society.

Non-Isothermal FIC

Li and coworkers used a similar experimental procedure but observed PLLA crystallization upon cooling. They determined that PLLA required a shear rate greater than 5 s⁻¹ to form cylindrites, and this rate was successfully employed by others to form "shish-like" crystals [55, 56]. This study also revealed that the cooling rate employed *while* the melt was experiencing shear, during non-isothermal crystallization, strongly influenced the resulting nucleation density, microstructure, and

ultimate percentage crystallinity. After experiencing a shear rate of 5 s-1, the PLLA did not crystallize if cooled at a rate of 5 K/min, but was able to crystallize to about 15% if cooled at 3 K/min and 42.36% when cooled at 1 K/min. Without shear, PLLA required a cooling rate less than 3 K/min to crystallize any measureable amount. The size and number of cylindrite-like crystals decreased with cooling rate, likely due to the relaxation of chain orientation in the melt.

In an effort to apply existing FIC theory to PLA melt flow and crystallization, Zhong and coworkers first established the rheological properties of the industrially-relevant Natureworks 4032D grade PLA, which contains 0.7 mol % L-isomeric content [35]. The longest reptation time and the Rouse time were estimated from the relaxation spectra, and this data was used to calculate the target shear rate and conditions required to initiate FIC. Using rotational rheology, the group monitored the onset of crystallization after shearing and confirmed that the critical shear rate to stretch the longest chains of this grade of PLA at 135 °C was 0.45 s-1. Above this rate, the crystallization process was greatly enhanced compared to the quiescent conditions, and the crystallization kinetics increased with increasing shear rate due to an increase in nucleation density. For a singular shear rate there was a critical shearing time required, and additional shearing time did not lead to faster crystallization kinetics under either isothermal or non-isothermal conditions.

Conditions to Create Shish Kebab Microstructure

Acknowledging the property enhancements that result from developing shish-kebab microstructure in PLA melt-manufactured product, Xu and coworkers developed two methods – one requiring a long shear step and a second requiring instead a quick shear pulse – to form this microstructure in PLLA. The first required an ultrasonic force to maintain energy input to an injection molded part until gate freeze, and as a result of the long exposure time to shear, several shish-kebabs were identified in the final molded samples [57]. However, under extensive shear, PLA will undergo a degradation mechanism that results in a loss of molecular weight [58]. To circumvent this degradation, a

short pulse of strong shear, such as 100 s^{-1} for 1 s, may also be used to induce shish-kebab structure. The shish created under such circumstances have been shown to be comprised of a higher conformational order than the surrounding kebabs or independently nucleated spherulites [36].

Crystallization under Continuous Shear

While most FIC investigations first subject the PLA melt to a shear flow and then observe the crystallization behavior and resulting morphology after the cessation of flow, PLA will also crystallize under a continuous shear flow. Yang and coworkers used an optical shear cell to first melt PLA to 200°C before cooling to 110°C, where the melt was then subject to a shear rate of 0.16 s^{-1} for 1500 seconds, or until crystallization was complete [59]. This continuous-shearing study was monitored by wide angle WAXD and POM. Results showed that both shish-kebabs and cylindrically stacked lamellae could form, survive and grow under flow provided the shear rate exceeded a critical rate. Weak continuous shear flow yielded more crystallinity while high shear rates reduced ultimate crystallinity.

Flow Induced Crystallization of Stereocomplex PLA

As described in section "Stereocomplex Crystallization", the SC of the L-isomer and D-isomer poly (lactic acid) co-crystallizing yields a SC crystalline structure that melts about 50 K higher than that of the PLLA homocrystal. The higher melting point of the SC crystal is of interest for commercial PLA formulations, because the ratio and microstructure of SC can be tailored to result in bulk properties competitive to traditional engineering thermoplastics. Because most engineering thermoplastics undergo some type of melt processing prior in the manufacture of industrial and consumer parts, the FIC of stereocomplex PLA has gained interest in recent years [60].

Pan and coworkers determined that in the absence of shear, the kinetics of HC formation, either L/L or D/D homocrystallization, are

more favorable than the formation of the SC crystal phase. However, several researchers have confirmed that shear flow increases the amount of SC crystal that forms in a PDLA/PLLA mixture [17]. In order to form SC crystals from the melt, D- and L- chains must at least partially mix and segments of D- and L- chains must align prior to crystallization, and a shearing promotes this phase mixing [61]. Bojda established that, for identical shearing conditions, PLA with 2.8% PDLA content crystallizes at a higher crystallization temperature upon cooling than does PLA with only 1.5% PDLA content, but during slow cooling both blends result in the same crystalline content[62]. Bai and coworkers determined the role of SC in the PLA melt by preparing a series of blends with increasing D-content. They discovered that, in low frequency melt behaviors of the blends, the slope of the storage modulus curve decreases with increasing D- content, indicating a slower relaxation of the melt with increasing D-content because the SC phase restrains the long-range motion of the PLLA chains in the melt [17].

To promote crystallization in the mixed phase, both increasing shear and decreasing the shearing temperature act to reduce chain mobility. Importantly, the molecular weights of both the PLLA and PDLA components drive the miscibility of the polymer blend in the melt, with blends displaying multiple melting peaks when molecular weights ranged from 23 – 50 kg/mol, but single melting behaviors if the PLLA and PLDA were of lower molecular weights. This is likely due to short chains in the melt having sufficient mobility to form SC, while longer chains are hampered by entanglement [63]. Song and coworkers studied equimolar blends of PDLA and PLLA to also determine that increasing shear rate prior to crystallization led to an increase in SC content [23]. As SC content increases, the α-crystal content formed by PLLA decreases accordingly. As confirmed by several researchers, the increased rate of crystallization is largely due to an increased number of SC nuclei that form under flow conditions. The increase in nucleation can be easily observed in the crystallized samples formed after flow, which contain many more and smaller spherulites relative to their quiescently-crystallized counterparts [60]. Increasing the pressure of a crystallizing PLA blend, however, promotes HC formation while suppressing SC formation, due to the reduced free volume of the melt [64].

Ultimately, the microstructure that results from flow-induced crystallization of PLA is a function of the material properties, shearing conditions, and crystallization temperature. One must exercise attention to detail when comparing results from the numerous studies in the literature, because a wide variety of conditions are reported for experimental setup. For example, both Bai and Xie studied the microstructure formed after flow-induced crystallization of similar PLLA/PDLA blends [17, 44]. Though both examined the microstructure after crystallization in the range of 160 °C, one study sheared the PLA at 100 s^{-1} for one second, while the second study sheared the PLA at 1 s^{-1} for 10 seconds. The sample experiencing the higher shear rate (but shorter duration) formed shish-kebab, anisotropic microstructure while the material experiencing the lower shear rate for a longer time interval formed many small spherulites. In order to fully promote the formation of the SC phase, Xu and coworkers pulled a glass fiber through the melt above the melting temperature of the HC, but below the melting temperature of the SC [65]. This technique enables the selective FIC of the stereocomplex under conditions which eliminate the possibility of HC forming. Physical testing after solidification revealed that the pull-out strength of the glass fiber embedded into the SC PLA was more than three times higher than a similar fiber embedded in an HC-rich, quiescently-crystallized sample of the same PLA.

Effects of Molecular weight and chain branching

Although, as mentioned above, under quiescent condition the molecular weight has a significant effect on the crystallization kinetics of PLA, the studies concerning this property on the flow induced crystallization are rare.

A. Jalali et al. [8] investigated the effect of shear rate and shear strain on the crystallization kinetics of PLA. They obtained two materials having the same D-LA content but a lower molecular weight than the starting sample by a hydrolysis procedure.

They found that the crystallization induction time decreased upon increasing the MW in the presence of the shear flow. This was ascribed to a longer relaxation time. They also found that shear flow promoted the formation of the α-phase at elevated temperature, 130° C, for all

different molecular weights. Furthermore, it was found that shear promoted the formation of the alpha phase below 100° C, namely at temperatures where the samples crystallized in quiescent conditions only showed the formation of the α'- phase. Finally, it was observed that shear induced the formation of cylindrite morphology only in high molecular weight PLA, whereas spherulitic morphology were developed for the low and medium molecular weight PLA in the same conditions.

Apart from the average molecular weight, the importance of the high molecular mass tails in polymer melt on the formation of oriented, anisotropic structures was pointed out by several researchers. For linear PLA a fast relaxation after shear takes place, which reduces the efficiency of shear flow in altering the nucleation ability and crystalline morphology. High molecular weight tails increase the relaxation time and thus drastically enhance the crystallization kinetics and the formation of the shish-kebab structure. Fang et al. [15] analyzed the effects of long chain branching, LCB, on the nucleation density enhancements and crystalline morphological evolution for shear-induced crystallization of PLA under isothermal conditions. They showed that LCB PLA crystallized much faster than linear PLA under the same shear conditions. In-situ POM observations demonstrated the LCB PLA not only presented a larger nucleation density for the same shear time, but also formed shish-kebab structures after being sheared for the sufficiently longer time.

Effects of fillers and nucleating agents

In many processes, deformation rates are applied on a PLLA melt containing nucleating agents. Many studies conducted on several polymers concluded that the contribution of nucleating agents and flow to nucleation density is often additive but can be synergistic.

Among nucleating agents for PLLA, the most common is talc [58]. Refaa et al. [66] investigated the effect of shear flow on pure PLA and on PLA with 5wt% of talc, evidencing a synergistic effect.

Though FIC of stereocomplex PLA phase has been discussed, the SC phase should also be highlighted as a true nucleating moiety for PLA crystallization. Wei et al. [67] investigated the crystallization behavior

of a PLLA/PDLA blend (99/1wt/wt) under shear to explore the combined effect of shear and stereocomplex crystallites on the crystallization rate of PLLA. As mentioned above, stereocomplex is probably the most efficient nucleating agent for PLA. Also in this case, the results showed that the crystallization rate of PLLA was synergistically accelerated by SC crystallites and shear. The authors ascribed this effect to a much slower relaxation behavior of PLLA/PDLA blend with respect to neat PLLA, possibly due to the crosslinking effect of SC crystallites.

Yin et al. [68] investigated the orientation and crystallization of PLLA combining the effect of nucleating agents and mechanical stretching. They combined both talc and stereocomplex. In particular, they used talc (1 wt%), PDLA (5 wt%) and also a combination of the two (1% of talc+5% of PDLA). During continuous uniaxial stretching at 75°C with a low stretching speed, nucleating agents remarkably enhance the crystallization of PLLA. It was found that the effect of the nucleating agents is dependent on the mechanically applied strain. At small strain, the crystallization of PLLA is remarkably enhanced by the nucleating agents. While at higher strain, the effect of the nucleating agents is obscured by the dominant effect of the strain-induced orientation on the crystallization of PLLA. The results are summarized in Figures 8 and 9.
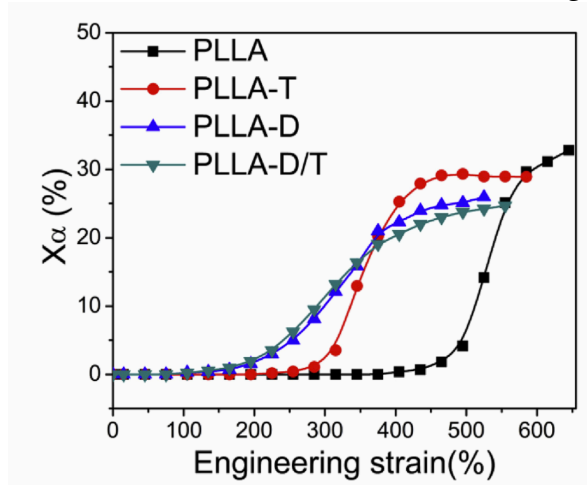

Figure 8 Development of a crystal in neat and nucleated PLLA as a function of engineering strain during uniaxial stretching at 75 °C. The stretching speed was 0.0125/s [68] Copyright 2015, Elsevier.
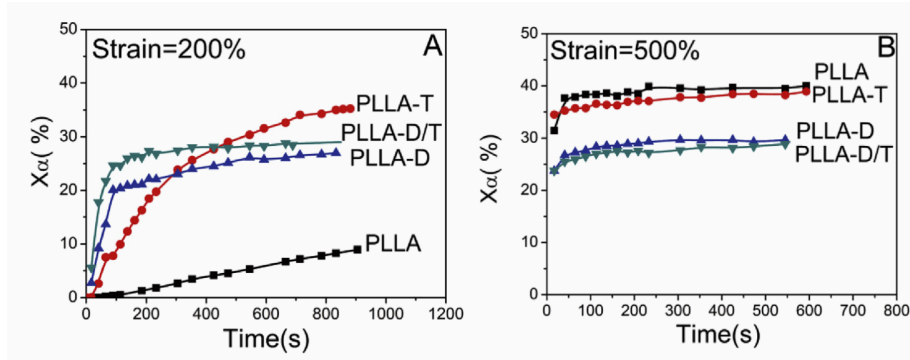
Figure 9 Variation of a crystal in neat and nucleated PLLA as a function of time during isothermal process at 75°C after step-stretching to 200% (A) and 500% (B), respectively [68]. Copyright 2015, Elsevier.

Tang et al. [69] considered the simultaneous effect of shear flow and Carbon Nanotubes (CNT), another quite effective nucleating agent for PLA [70]. The results show more than an additive effect of CNTs and shear flow on enhancing crystallization of PLA in nonisothermal conditions.

The synergic effect was attributed to the extra nucleating sites produced by the interplay of shear flow and CNTs. The authors ascribed the origin of these extra sites to the anchoring effect of CNTs on shear-induced crystallization of PLA and suppressing effect of CNTs on the relaxation of shear-induced nuclei. By using oscillatory shear injection-molding technique on samples loaded with 0.1wt% of CNTs, the authors obtained samples with a crystallinity degree of more than 20% in the whole thickness, whereas the samples made of pure PLA presented a percentage of about 15% at the skin and were essentially amorphous in the core (Figure 10).

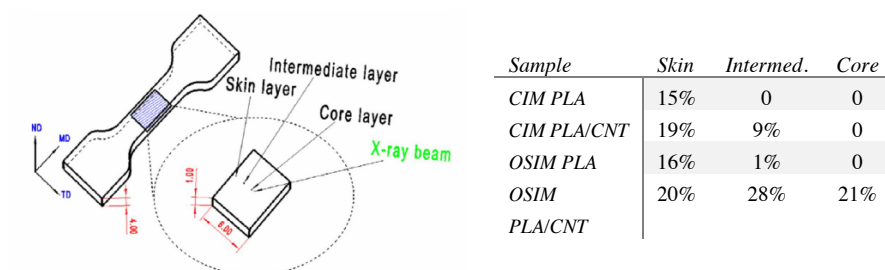| Sample	Skin	Intermed.	Core
CIM PLA	15%	0	0
CIM PLA/CNT	19%	9%	0
OSIM PLA	16%	1%	0
OSIM PLA/CNT	20%	28%	21%

Figure 10 Crystallinity in different positions (as indicated in the left figure – measures in mm) for samples made by Conventional Injection Molding (CIM) and oscillatory shear injection-molding (OSIM) with and without CNT [69]. Copyright 2012, American Chemical Society.

Different results are reported by Xie et al. [71], who studied the crystallinity distribution in molded PLLA samples containing 0.05% of CNT and in molded PLLA samples containing 5% of SC, and noticed that the promoting effect on crystallization of PLLA by intense shear flow was so significant that the nucleation effect of nucleating agents CNT and SC could be neglected. On the contrary, the addition of nucleating agent resulted in a decreased crystallinity of PLLA at high mold temperature (higher than Tg). This result was ascribed to the spatial restriction of the chain segment folding into the lattice and formation of less perfect crystals.

A synergistic effect of CNT and deformation was assessed in extensional flow by Li et al. [72]. By applying intense extensional flow on PLA melt containing 0.3wt% of CNT, they obtained two types of special aligned crystalline microstructures (shish): homogeneous crystalline fibrils only consisting of PLA extended chains; hybrid crystalline fibrils characterized by CNTs coated with PLA extended chain as depicted in Figure 11.
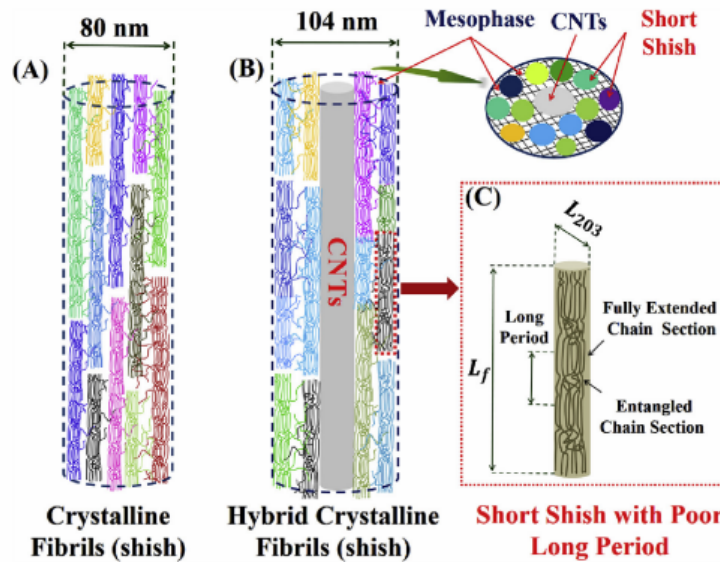
Figure 11. (A), (B) schematic drawing showing the multiple short length shish in neat PLA, CNT/PLA nanocomposite, respectively. (C) schematic illustration of molecular arrangement in the short length shish. The extensional flow direction is vertically. [62] Copyright 2016, Elsevier.

FIC in PLA processing

PLLA can be processed by most of the conventional techniques for thermoplastics [73, 74]. The change imparted to PLLA during melt processing is more than simply creating the net shape of a PLLA part. Changes imparted by melt flow, including chain orientation, crystallization and degradation, may result in substantial changes to mechanical properties. In 2010, Carrasco and coworkers detailed both the chain degradation and the improvement in mechanical properties that were attributed to injection molding and annealing a PLA with 4.25% D content [75]. Simply injection molding the PLA did not induce crystallization because of the fast cooling time, but it did allow for PLA chains to orient and then crystallize in a subsequent annealing step. The impressive property improvements induced by crystallization during annealing are shown in Table 3.

Table 3. Mechanical properties of injection molded tensile bars produced from PLA containing 4.25% D content, as molded and after annealing [75].

	As Injection Molded	Post-Annealing
% Crystallinity	< 1%	33%
Youngs modulus (E) (GPa)	3.7	4.1
Yield strength (σ_y) (MPa)	65.6	75.4
Elongation at break (%)	4.0	2.5

Like most studies reported in the literature, Carrasco and coworkers did not directly discuss or quantify FIC as a driving force for crystalline development in the samples described above. However, the high flow rate and resulting polymer orientation inherent in the injection molding process provide optimal conditions for FIC to occur, and the mechanical property results indicate that the annealing process was very efficient after melt flow, orientation and solidification. Therefore, in the following we review the studies reporting processing techniques that show evidence of flow-induced crystallization.

Injection molding and related processes

Considering the fast cooling rates involved in injection molding, PLLA should not crystallize at all if just the quiescent crystallization kinetics are considered. Despite of this, several literature works report non-negligible crystallinity degrees in injection molded PLLA parts. Gosh et al. [76] for instance, obtained injection molded samples of a PLLA homopolymer in several different molding conditions (according to a design of experiments array) and found a non-negligible overall crystallinity degree (up to about 6%) in the 2mm thick samples. They observed that this crystallinity content increased on increased the maximum shear stress, clearly evidenced a phenomenon of flow-induced crystallization. This observation is consistent with the results reported in the paper by Tang et al. [69] mentioned above: the authors observe that in injection molded parts the skin region is more crystalline than the core, which can be justified only by an effect of flow-induced crystallization since the cooling rates are higher at the skin and lower at the core.

It is important to note that for PLLA grades with significant amount of D-lactide, injection molded parts are reported to be amorphous [77], and only special molding protocols can provide crystalline samples [78, 79]. This suggests that the enhancement effect on crystallization due to flow could be not enough to compensate the high cooling rates.

In order to obtain molded samples with a higher degree of crystallization, some variants of the conventional injection molding (CIM) were applied to PLA. The shear-controlled orientation injection molding (SCORIM) technique is based on a device that is attached to the injection nozzle and is composed of a hot runner circuit that divides the melt stream into two channels where two hydraulically actuated pistons are operated during the holding pressure stage. Compared to CIM, where the molten material solidifies under the influence of an almost static pressure, in SCORIM the polymer melt is continuously displaced inside the mold cavity by the action of the hydraulic pistons. This causes, as the solidification takes place progressively from the skin to core regions, a continuous shear imposed to the melt, with a considerable enhancement of flow-induced crystallization effects.

Altpeter et al. [80] compared the results obtained in terms of crystallinity in PLLA samples molded with CIM and SCORIM. They found that the degree of crystallinity was higher than 20% for the SCORIM and about 5% for the conventional sample. They also found that the crystalline structure of SCORIM processed moldings were highly oriented.

The authors also report optical images of the molded samples (reproduced in Figure 12), from which it is clear that samples obtained by CIM are transparent, whereas samples obtained by SCORIM present an opaque skin layer due to a significant crystalline degree.
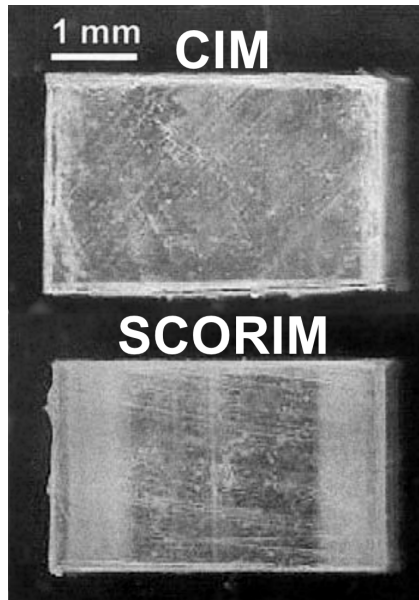
Figure 12. Optical images of samples obtained by Conventional Injection Molding (CIM) and SCORIM (adapted from [80]). Copyright 2004, Springer Nature.

Ghosh et al [81] analyzed the effect of several processing conditions on SCORIM, and compared the results with CIM. Concerning the morphology, the authors noticed that the samples obtained by SCORIM presented a core-free morphology, in contrast to the skin-core morphology of CIM. The extent of core-fibrillation increased with shearing time. The authors noticed that all the SCORIM processed PLLA exhibited higher toughness and higher maximum stress compared with CIM processed PLLA.

Another technique based on SCORIM is the so-called oscillatory shear injection molding (OSIM). Similarly, to SCORIM, in OSIM there are two hydraulically actuated pistons to generate a shear stress field during the cooling solidification of melt in the cavity. Contrasting to SCORIM where the multi-piston oscillating packing unit is an independent device, in OPIM a hot runner system is adopted, combined to a double live-feed device to injection molding machine. This greatly improves the SCORIM device.

Xie et al. [71] measured the crystallinity profile inside PLLA (D-Lactide content 0.4wt%) samples obtained by CIM and OSIM. They observed that, with a mold temperature of 40°C, in CIM the samples

were completely amorphous whereas in OSIM the crystallinity degree was as high as 40% up to about 500 micron from the skin (the core was amorphous). The authors found an increase of the Vicat softening temperature in the OSIM processed samples. Similar results are also reported by Sang et al. [82], who also noticed an improvement of Young's modulus and tensile strength in OSIM processed samples with respect to CIM processed samples.

Foam injection molding

Foam injection molding is a process to make parts having better dimensional stability with less material and a faster production cycle with respect to the conventional injection molding process. A physical blowing agent mixed with the polymer melt allows the reduction of the processing temperatures due to its plasticization effect that reduces the melt viscosity. This is a great advantage for the processing of PLA, well-known for its thermal sensibility and narrow processing window.

The dissolution of both CO_2 [83, 84] and N_2 [85] in PLA enhances the crystallization kinetics in quiescent conditions. It is reported in the literature [86, 87], that the presence of CO_2 and biaxial stretching during foaming can both significantly increase the PLA crystallization rate, so that detectable crystallization content (approximately 10%) are found in foam injection molded parts [10], despite the fast cooling rates experienced by the material during processing.

Extrusion-casting

A study of the effect of flow rate during extrusion was conducted by Tabatabei and Park [84]. They found that the PLA crystallization during extrusion could be promoted by flow at a temperature higher than the melting point.

Biaxially stretching extruded films were proved to be an effective method to develop the final crystallinity of PLA. Yu et al. [88] reported that stretching of a melt drawn PLA film induces crystallization. Ching-

Chun Tsai et al. [89] also report a study on the effect of stress-induced nucleation on the crystallization behavior of films of PLA.

Houichi et al [90] carried out a study on the crystallization kinetics and spherulitic morphology of poly (lactic acid) induced by casting process. They found that that the rate of cold crystallization was sharply increased with draw ratio.

Melt spinning

The deformation rates during melt spinning are very high, and thus it is expected that flow-induced crystallization plays a significant role during this process. Several studies about the PLA melt-spinning process showed that the crystallinity considerably increased on increasing the melt-draw ratio (MDR) [91]. Cicero et al. [45] and Fambri et al [92] found an increase of crystallinity (from 0% to 51%) either on increasing the draw ratio or on decreasing the draw temperature.

Shim et al [93] analyzed the effects of a spinning speed in the range 1000-4000 m/min on a PLLA with 2wt% D-content. They found a linear increase of crystallinity with the speed, until a value of 25% at 4000m/min). Similar results were found by Schmack et al. [91] adopting a PLA with a lower content of L-lactide (92wt%).

Hossain et al [94] related the crystallinity of the spun fiber to the diameter of the fiber. They found a significant increase of crystallinity, and of the crystal size of the fiber, on decreasing the fiber diameter, and on increasing the orientation.

Additive / Fused Filament Deposition Modeling

At present, PLA represents one of the most common materials used for the Fused Filament Deposition Modeling type of additive manufacturing. In this technique, a solid filament of PLA is fed through a small heated extruder head, which laterally traverses a solid surface while the molten polymer is "pushed" out of the extruder nozzle and deposited on the build surface. While the nozzle diameter is constant, several process parameters can be modified that logically influence the crystallization of PLA after printing. Specifically, melt temperature, printing speed, and the temperature of the build plate dictate the

viscosity, cooling rate, and shear rate experienced by the PLA during printing. Therefore, it is logical that FIC may occur if the thermal and flow conditions of the printing process are properly manipulated.

Indications in this directions were recently found by applying in-situ Ra- man spectroscopy to Fused Filament Deposition experiments conducted with a polycaprolactone [95]. McIlroy and Graham [96] made an attempt to model polymer stretch and orientation during typical non-isothermal Fused Filament Fabrication flow, and to determine the conditions under which flow-enhanced nucleation can occur due to residual stretch. To date, however, no results have been reported that calculate the development of specific work for PLA during the printing process and therefore no direct evidence exists as such.

However, several studies have confirmed the relationship between PLA printing conditions and final printed part properties. Though several different grades of PLA were used for the various investigations, results consistently suggest that minimizing the printed layer height frequently results in the highest tensile properties of a printed part [97]. While the print pattern also drives stress propagation during tensile or torsional deformation, the importance of developing crystallinity in printed PLA is beginning to emerge. Layer height and build plate temperature have proven to be important variable that influence the development of PLA crystallinity. While not defined as "FIC" in the literature, the results of Gardner and coworkers certainly fit the description of FIC [98]. When printing PLA, they discovered that, if all other variables are held constant and the build plate was held at high temperature (160 °C), a 0.2 mm layer height contained *more, smaller spherulites* than the sample produced with a 0.4 mm layer height. This PLA printed in a 0.2 mm layer height would be, all else the same, subject to higher shear rate than the 0.4 mm counterpart, resulting in an increased nucleation density and ultimate higher percentage of crystalline content, both indicative of FIC. Similarly, Chacón and coworkers found that a thin printed layer thickness combined with a high feed rate are recommended for optimal strength and stiffness [99]. However, the development of good interfacial strength between the printed layers and the resulting interfacial mechanical property development may suffer with increasing PLA crystallization. In a subsequent study, Wang and Gardner [98] confirmed that, as a result of PLA densification due to crystallization at the interface, voids form that

ultimately decrease interfacial strength. This serves as a good reminder that one must consider the future mechanical loading of a printed part and design the printing strategy accordingly, maximizing tensile strength in the direction of printing in the anticipation of tensile loading, and maximizing interfacial strength if torsional loads are expected.

Conclusions

The enhancing effect of flow field on the crystallization kinetics of PLLA has been assessed by several literature works. This phenomenon is obviously extremely significant for engineering applications, which require the melt processing of PLA to produce final parts and demand increasingly custom property profiles, often with the goal of maximizing mechanical properties or controlling the degradation rate of the final thermoplastic product. The state of the art suggests that to achieve a high degree of control and precision, the influence of the PLA properties such as isomer content, molecular weight, and branching must be considered to design proper melt processing conditions that result in controlled flow-induced crystallization and, ultimately, predictable PLA microstructure. In spite of all these studies, all the effects remain phenomenological, and a comprehensive and systematic understanding is not yet complete. Therefore, ongoing studies must continue to develop these complex relationships before engineering predictable PLA microstructure development becomes commonplace.

References

1.   Roozemond PC, van Drongelen M, Peters GWM (2016) Modeling Flow-Induced Crystallization. Springer Berlin Heidelb. doi: 10.1007/12_2016_351
2.   Pantani R, De Santis F, Sorrentino A, De Maio F, Titomanlio G (2010) Crystallization kinetics of virgin and processed poly(lactic acid). Polym Degrad Stab 95:1148–1159 . doi: 10.1016/j.polymdegradstab.2010.04.018
3.   Androsch R, Schick C, Lorenzo ML Di (2017) Kinetics of Nucleation and Growth of Crystals of Poly(l-lactic acid). Adv Polym Sci 279:235–272 . doi: 10.1007/12_2016_13
4.   Eling B, Gogolewski S, Pennings AJ (1982) Biodegradable

materials of poly(l-lactic acid): 1. Melt-spun and solution-spun fibres. Polymer (Guildf) 23:1587–1593 . doi: 10.1016/0032-3861(82)90176-8

5. Cartier L, Okihara T, Ikada Y, Tsuji H, Puiggali J, Lotz B (2000) Epitaxial crystallization and crystalline polymorphism of polylactides. Polymer (Guildf) 41:8909–8919 . doi: 10.1016/S0032-3861(00)00234-2

6. Saeidlou S, Huneault MA, Li H, Park CB (2012) Poly(lactic acid) crystallization. Prog Polym Sci 37:1657–1677 . doi: 10.1016/j.progpolymsci.2012.07.005

7. Garlotta D (2001) A literature review of poly(lactic acid). J Polym Environ 9:63–84 . doi: 10.1023/A:1020200822435

8. Jalali A, Huneault MA, Elkoun S (2017) Effect of molecular weight on the nucleation efficiency of poly(lactic acid) crystalline phases. J Polym Res 24: . doi: 10.1007/s10965-017-1337-x

9. De Meo A, De Santis F, Pantani R (2018) Dynamic local temperature control in micro-injection molding: Effects on poly(lactic acid) morphology. Polym Eng Sci 58:586–591 . doi: 10.1002/pen.24784

10. Volpe V, De Filitto M, Klofacova V, De Santis F, Pantani R (2018) Effect of mold opening on the properties of PLA samples obtained by foam injection molding. Polym Eng Sci 58:475–484 . doi: 10.1002/pen.24730

11. Zaldua N, Mugica A, Zubitur M, Iturrospe A, Arbe A, Re G Lo, Raquez J-M, Dubois P, Müller AJ (2016) The role of PLLA- g - montmorillonite nanohybrids in the acceleration of the crystallization rate of a commercial PLA. CrystEngComm 18:9334–9344 . doi: 10.1039/C6CE02005D

12. Tsuji H, Sugiura Y, Sakamoto Y, Bouapao L, Polymer I-S (2008) Crystallization behavior of linear 1-arm and 2-arm poly (l-lactide) s: effects of coinitiators. Polymer (Guildf) 49:1385–1397 . doi: 10.1016/j.polymer.2008.01.029

13. Aziz AA, Hay JN, Jenkins MJ (2018) The melting of Poly (L-Lactic acid). Eur Polym J. doi: 10.1016/j.eurpolymj.2018.01.041

14. Wang J, Bai J, Zhang Y, Fang H, Wang Z (2016) Shear-induced enhancements of crystallization kinetics and morphological

transformation for long chain branched polylactides with different branching degrees . Sci Rep 6:26560 . doi: 10.1038/srep26560

15. Fang H, Zhang Y, Bai J, Wang Z (2013) Shear-Induced Nucleation and Morphological Evolution for Bimodal Long Chain Branched Polylactide. Macromolecules 46:6555–6565 . doi: 10.1021/ma4012126

16. Nam J, Ray S, Okamoto M (2003) Crystallization Behavior and Morphology of Biodegradable {Polylactide/Layered} Silicate Nanocomposite. Macromolecules 36:7126–7131 . doi: 10.1021/ma034623j

17. Bai J, Wang J, Wang W, Fang H, Xu Z, Chen X, Wang Z (2016) Stereocomplex Crystallite-Assisted Shear-Induced Crystallization Kinetics at a High Temperature for Asymmetric Biodegradable PLLA/PDLA Blends. ACS Sustain Chem Eng 4:273–283 . doi: 10.1021/acssuschemeng.5b01110

18. De Santis F, Pantani R, Santis F (2013) Nucleation density and growth rate of polypropylene measured by calorimetric experiments. J Therm Anal Calorim 112:1–10 . doi: 10.1007/s10973-012-2732-5

19. Li S, Hu Y (2014) Chapter 2. Polylactide Stereo-complex: From Principles to Applications. pp 37–65

20. Rahman N, Kawai T, Matsuba G, Nishida K, Kanaya T, Watanabe H, Okamoto H, Kato M, Usuki A, Matsuda M, Nakajima K, Honma N (2009) Effect of Polylactide Stereocomplex on the Crystallization Behavior of Poly(L-lactic acid). Macromolecules 42:4739–4745 . doi: 10.1021/ma900004d

21. Zou G, Qu X, Zhao C, He Y, Li J (2018) Self-Nucleation Efficiency of PDLA in PLAs: Crystallization Behavior and Morphology. Polym Sci Ser A 60:206–214 . doi: 10.1134/S0965545X18020165

22. Schmidt SC, Hillmyer MA (2001) Polylactide stereocomplex crystallites as nucleating agents for isotactic polylactide. J Polym Sci Part B Polym Phys 39:300–313 . doi: 10.1002/1099-0488(20010201)39:3<300::AID-POLB1002>3.0.CO;2-M

23. Song Y, Zhang X, Yin Y, de Vos S, Wang R, Joziasse CAP, Liu G, Wang D (2015) Enhancement of stereocomplex formation in

poly(l-lactide)/poly(d-lactide) mixture by shear . Elsevier Ltd 72 IS-: . doi: 10.1016/j.polymer.2015.07.023

24. Fukushima K, Kimura Y (2006) Stereocomplexed polylactides {(Neo-PLA)} as high-performance bio-based polymers: their formation, properties, and application. Polym Int 55:626–642 . doi: 10.1002/pi.2010

25. Ikada Y, Jamshidi K, Tsuji H, Hyon S (1987) Stereocomplex formation between enantiomeric poly(lactides). 20:904–906 . doi: 10.1021/ma00170a034

26. Farah S, Anderson DG, Langer R (2016) Physical and mechanical properties of PLA, and their functions in widespread applications — A comprehensive review. Adv Drug Deliv Rev 107:367–392 . doi: 10.1016/j.addr.2016.06.012

27. Van De Velde K, Kiekens P (2002) Biopolymers: Overview of several properties and consequences on their applications. Polym Test 21:433–442 . doi: 10.1016/S0142-9418(01)00107-6

28. Ma Z, Balzano L, Portale G, Peters GWM (2014) Flow induced crystallization in isotactic polypropylene during and after flow . Elsevier Ltd 55: . doi: 10.1016/j.polymer.2014.09.039

29. Flory PJ (1949) Thermodynamics of Crystallization in High Polymers. IV. A Theory of Crystalline States and Fusion in Polymers, Copolymers, and Their Mixtures with Diluents. J Chem Phys 17:223–240 . doi: 10.1063/1.1747230

30. Flory PJ (1947) Thermodynamics of Crystallization in High Polymers II. Simplified Derivation of Melting-Point Relationships. J Chem Phys 15:684–684 . doi: 10.1063/1.1746627

31. Flory PJ (1947) Thermodynamics of Crystallization in High Polymers. I. Crystallization Induced by Stretching. J Chem Phys 15:397–408 . doi: 10.1063/1.1746537

32. Wang Z, Ma Z, Li L (2016) Flow-Induced Crystallization of Polymers: Molecular and Thermodynamic Considerations. Macromolecules 49:1505–1517 . doi: 10.1021/acs.macromol.5b02688

33. Meerveld J van, Peters GWM, Hütter M (2004) Towards a rheological classification of flow induced crystallization experiments of polymer melts . Rheol Acta 44:119–134 . doi: 10.1007/s00397-004-0382-7

34. Housmans R. J. A.; Roozemond, P. C.; Peters, G. W. M.; Meijer, H. E. H. JW. S (2009) Saturation of Pointlike Nuclei and the Transition to Oriented Structures in Flow-Induced Crystallization of Isotactic Polypropylene. Macromolecules 42:5728–5740 . doi: 10.1021/ma802479c

35. Zhong Y, Fang H, Zhang Y, Wang Z, Yang J, Wang Z (2013) Rheologically Determined Critical Shear Rates for Shear-Induced Nucleation Rate Enhancements of Poly(lactic acid) . ACS Sustain Chem Eng 1:663–672 . doi: 10.1021/sc400040b

36. Xu H, Xie L, Hakkarainen M (2015) Beyond a Model of Polymer Processing-Triggered Shear: Reconciling Shish-Kebab Formation and Control of Chain Degradation in Sheared Poly(l-lactic acid). ACS Sustain Chem Eng 3:1443–1452 . doi: 10.1021/acssuschemeng.5b00320

37. Cui K, Ma Z, Tian N, Su F, Liu D, Li L (2018) Multiscale and Multistep Ordering of Flow-Induced Nucleation of Polymers. Chem Rev 118:1840–1886 . doi: 10.1021/acs.chemrev.7b00500

38. Seo J, Takahashi H, Nazari B, Rhoades AM, Schaake RP, Colby RH (2018) Isothermal Flow-Induced Crystallization of Polyamide 66 Melts. Macromolecules 51:4269–4279 . doi: 10.1021/acs.macromol.8b00082

39. Mykhaylyk OO, Chambon P, Graham RS, Fairclough JPA, Olmsted PD, Ryan AJ (2008) The Specific Work of Flow as a Criterion for Orientation in Polymer Crystallization. Macromolecules 41:1901–1904 . doi: 10.1021/ma702603v

40. Rhoades AM, Gohn AM, Seo J, Androsch R, Colby RH (2018) Sensitivity of Polymer Crystallization to Shear at Low and High Supercooling of the Melt. Macromolecules 51:2785–2795 . doi: 10.1021/acs.macromol.8b00195

41. Somani RH, Hsiao BS, Nogales A, Fruitwala H, Srinivas S, Tsou AH (2001) Structure Development during Shear Flow Induced Crystallization of i-PP: In Situ Wide-Angle X-ray Diffraction Study. Macromolecules 34:5902–5909 . doi: 10.1021/ma0106191

42. Somani Hsiao, B.S., Nogales, A., Srinivas, S., Tsou, A.H., Sics, I., Balta-Calleja, F.J. and Ezquerra, T.A. RH (2000) Structure development during shear flow-induced crystallization of i-PP: in-situ small-angle X-ray scattering study. Macromolecules

33:9385–9394 . doi: 10.1021/ma001124z

43. Liu G, Zhang X, Wang D (2014) Tailoring Crystallization: Towards High-Performance Poly(lactic acid). Adv Mater 26:6905–6911 . doi: 10.1002/adma.201305413

44. Xie L, Xu H, Li Z-M, Hakkarainen M (2016) Structural Hierarchy and Polymorphic Transformation in Shear-Induced Shish-Kebab of Stereocomplex Poly(Lactic Acid). Macromol Rapid Commun 37:745–751 . doi: 10.1002/marc.201500736

45. Cicero JA, Dorgan JR, Janzen J, Garrett J, Runt J, Lin JS (2002) Supramolecular morphology of two-step, melt-spun poly(lactic acid) fibers. J Appl Polym Sci 86:2828–2838 . doi: 10.1002/app.11267

46. Cicero JA, Dorgan JR, Garrett J, Runt J, Lin JS (2002) Effects of molecular architecture on two-step, melt-spun poly(lactic acid) fibers. J Appl Polym Sci 86:2839–2846 . doi: 10.1002/app.11268

47. Gupta B, Revagade N, Hilborn J (2007) Poly(lactic acid) fiber: An overview. Prog Polym Sci 32:455–482 . doi: 10.1016/j.progpolymsci.2007.01.005

48. Solarski S, Ferreira M, Devaux E (2005) Characterization of the thermal properties of PLA fibers by modulated differential scanning calorimetry. Polymer (Guildf) 46:11187–11192 . doi: 10.1016/j.polymer.2005.10.027

49. Barham P, Keller A (1975) A criterion for distinguishing between polymer fibers of fundamentally different origin. J Polym Sci Polym Lett Ed 13:197–202 . doi: 10.1002/pol.1975.130130402

50. Mahendrasingam A, Blundell DJ, Parton M, Wright AK, Rasburn J, Narayanan T, Fuller W (2005) Time resolved study of oriented crystallisation of poly(lactic acid) during rapid tensile deformation. Polymer (Guildf) 46:6009–6015 . doi: 10.1016/j.polymer.2005.05.081

51. Fitz BD, Jamiolkowski DD, Andjeli S (2002) Tg Depression in poly (L (-)-lactide) crystallized under partially constrained conditions. Macromolecules 35:5869–5872

52. Pogodina NV, Winter HH, Srinivas S (1999) Strain effects on physical gelation of crystallizing isotactic polypropylene. J Polym Sci Part B Polym Phys 37:3512–3519 . doi:

10.1002/(SICI)1099-0488(19991215)37:24<3512::AID-POLB12>3.0.CO;2-#

53. Li X, Li Z, Zhong G-J, Li L-B (2008) Steady–shear-induced Isothermal Crystallization of Poly(<scp>L</scp> -lactide) (PLLA). J Macromol Sci Part B 47:511–522 . doi: 10.1080/00222340801955313

54. Huang S, Li H, Jiang S, Chen X, Polymer A-L (52AD) Crystal structure and morphology influenced by shear effect of poly (L-lactide) and its melting behavior revealed by WAXD, DSC and in-situ POM. Polymer (Guildf) 15:3487 . doi: 10.1016/j.polymer.2011.05.044

55. Li X, Zhong G, Li Z (2010) Non-isothermal crystallization of poly(L-lactide) (PLLA) under quiescent and steady shear conditions. Chinese J Polym Sci 28:357–366 . doi: 10.1007/s10118-010-9015-z

56. Yamazaki S, Itoh M, Oka T, Journal K-K (2010) Formation and morphology of "shish-like" fibril crystals of aliphatic polyesters from the sheared melt. Eur Polym J 46:58–68 . doi: 10.1016/j.eurpolymj.2009.09.003

57. Xu H, Zhong G-J, Fu Q, Lei J, Jiang W, Hsiao BS, Li Z-M (2012) Formation of Shish-Kebabs in Injection-Molded Poly(l-lactic acid) by Application of an Intense Flow Field . ACS Appl Mater Interfaces 4:6774–6784 . doi: 10.1021/am3019756

58. De Santis F, Pantani R (2015) Melt compounding of poly (Lactic Acid) and talc: assessment of material behavior during processing and resulting crystallization. J Polym Res 22:242 . doi: 10.1007/s10965-015-0885-1

59. Yang I-K, Wu C-H (2014) Real-time SAXS measurements and rheological behavior of poly(lactic acid) crystallization under continuous shear flow. J Polym Res 21:609 . doi: 10.1007/s10965-014-0609-y

60. Bai H, Deng S, Bai D, Zhang Q, Fu Q (2017) Recent Advances in Processing of Stereocomplex-Type Polylactide. Macromol Rapid Commun 38:1700454 . doi: 10.1002/marc.201700454

61. Hemmi K, Matsuba G, Tsuji H, Kawai T, Kanaya T, Toyohara K, Oda A, Endou K (2014) Precursors in stereo-complex crystals of poly(L-lactic acid)/poly(D-lactic acid) blends under shear flow. J Appl Crystallogr 47:14–21 . doi:

10.1107/S1600576713031907

62. Bojda J, Piorkowska E (2016) Shear-induced nonisothermal crystallization of two grades of PLA. Polym Test 50:172–181 . doi: 10.1016/j.polymertesting.2016.01.006

63. Shao J, Xiang S, Bian X, Sun J, Li G, Chen X (2015) Remarkable melting behavior of PLA stereocomplex in linear PLLA/PDLA blends. Ind Eng Chem Res 54:2246–2253 . doi: 10.1021/ie504484b

64. Song Y, Zhao Q, Yang S, Ru J, Lin J, Xu J, Lei J, Li Z (2018) Flow-induced crystallization of polylactide stereocomplex under pressure. J Appl Polym Sci 135:46378 . doi: 10.1002/app.46378

65. Xu J-Z, Li Y, Li Y-K, Chen Y-W, Wang R, Liu G, Liu S-M, Ni H-W, Li Z-M (2018) Shear-induced stereocomplex cylindrites in polylactic acid racemic blends: Morphology control and interfacial performance . Polymer (Guildf) 140:179–187 . doi: 10.1016/j.polymer.2018.02.048

66. Refaa Z, Boutaous M, Xin S, Fulchiron R (2017) Synergistic effects of shear flow and nucleating agents on the crystallization mechanisms of Poly (Lactic Acid). J Polym Res 24:18 . doi: 10.1007/s10965-016-1179-y

67. Wei X-F, Bao R-Y, Gu L, Wang Y, Ke K, Yang W, Xie B-H, Yang M-B, Zhou T, Zhang A-M (2014) Synergistic effect of stereocomplex crystals and shear flow on the crystallization rate of poly(L-lactic acid): A rheological study. RSC Adv 4:2733–2742 . doi: 10.1039/C3RA45402A

68. Yin Y, Zhang X, Song Y, de Vos S, Wang R, Joziasse CAP, Liu G, Wang D (2015) Effect of nucleating agents on the strain-induced crystallization of poly(l-lactide). Polymer (Guildf) 65:223–232 . doi: 10.1016/j.polymer.2015.03.061

69. Tang H, Chen J-B, Wang Y, Xu J-Z, Hsiao BS, Zhong G-J, Li Z-M (2012) Shear Flow and Carbon Nanotubes Synergistically Induced Nonisothermal Crystallization of Poly(lactic acid) and Its Application in Injection Molding . Biomacromolecules 13:3858–3867 . doi: 10.1021/bm3013617

70. Xu J, Chen T, Yang C, Li Z, Mao Y, Zeng B, Hsiao B (2010) Isothermal Crystallization of Poly(L-lactide) Induced by Graphene Nanosheets and Carbon Nanotubes: A Comparative Study. Macromolecules 43:5000–5008 . doi:

10.1021/ma100304n

71. Xie X-L, Sang Z-H, Xu J-Z, Zhong G-J, Li Z-M, Ji X, Wang R, Xu L (2017) Layer structure by shear-induced crystallization and thermal mechanical properties of injection-molded poly(l-lactide) with nucleating agents . Polymer (Guildf) 110:196–210 . doi: 10.1016/j.polymer.2017.01.004

72. Li C, Guo J, Jiang T, Zhang X, Xia L, Wu H, Guo S, Zhang X (2018) Extensional flow-induced hybrid crystalline fibrils (shish) in CNT/PLA nanocomposite. Carbon N Y 129:720–729 . doi: https://doi.org/10.1016/j.carbon.2017.12.063

73. Avolio R, Castaldo R, Avella M, Cocca M, Gentile G, Fiori S, Errico ME (2018) PLA-based plasticized nanocomposites: Effect of polymer/plasticizer/filler interactions on the time evolution of properties. Compos Part B Eng 152:267–274 . doi: 10.1016/j.compositesb.2018.07.011

74. Kühnert I, Spörer Y, Brünig H, Tran NHA, Rudolph N (2017) Processing of Poly(lactic Acid). In: Di Lorenzo M, Androsch R (eds) Industrial Applications of Poly(lactic acid). Springer, pp 1–33

75. Carrasco F, Pagès P, Gámez-Pérez J, Santana OO, Maspoch ML (2010) Processing of poly(lactic acid): Characterization of chemical structure, thermal stability and mechanical properties. Polym Degrad Stab 95:116–125 . doi: 10.1016/j.polymdegradstab.2009.11.045

76. Ghosh S, Viana JC, Reis RL, Mano JF (2007) Effect of processing conditions on morphology and mechanical properties of injection-molded poly(l-lactic acid). Polym Eng Sci 47:1141–1147 . doi: 10.1002/pen.20799

77. Pantani R, Sorrentino A (2013) Influence of crystallinity on the biodegradation rate of injection-moulded poly(lactic acid) samples in controlled composting conditions. Polym Degrad Stab 98:1089–1096 . doi: 10.1016/j.polymdegradstab.2013.01.005

78. De Santis F, Volpe V, Pantani R (2017) Effect of molding conditions on crystallization kinetics and mechanical properties of poly(lactic acid). Polym Eng Sci 57:306–311 . doi: 10.1002/pen.24414

79. Harris AM, Lee EC (2007) Improving mechanical performance

of injection molded PLA by controlling crystallinity . Wiley Subscr Serv Inc, A Wiley Co 107: . doi: 10.1002/app.27261

80. Altpeter H, Bevis MJ, Grijpma DW, Feijen J (2004) Non-conventional injection molding of poly(lactide) and poly(epsilon-caprolactone) intended for orthopedic applications. J Mater Sci Mater Med 15:175–184 . doi: 10.1023/B:JMSM.0000011820.64572.a5

81. Ghosh S, Viana JC, Reis RL, Mano JF (2008) Oriented morphology and enhanced mechanical properties of poly(l-lactic acid) from shear controlled orientation in injection molding. Mater Sci Eng A 490:81–89 . doi: 10.1016/j.msea.2008.01.003

82. Sang Z-H, Chen Y, Li Y, Xu L, Lei J, Yan Z, Zhong G-J, Li Z-M (2018) Simultaneously improving stiffness, toughness, and heat deflection resistance of polylactide using the strategy of orientation crystallization amplified by interfacial interactions. Polym Cryst 1:e10004 . doi: 10.1002/pcr2.10004

83. Sankarpandi S, Park CB, Ghosh AK (2017) CO_2 -induced crystal engineering of polylactide and the development of a polymeric nacreous microstructure. Polym Int 66:1587–1597 . doi: 10.1002/pi.5417

84. Tabatabaei A, Park CB (2017) In-situ visualization of PLA crystallization and crystal effects on foaming in extrusion . Eur Polym J 96:505–519 . doi: 10.1016/j.eurpolymj.2017.09.026

85. Ameli A, Nofar M, Jahani D, Rizvi G, Park CB (2015) Development of high void fraction polylactide composite foams using injection molding: Crystallization and foaming behaviors. Chem Eng J 262:78–87 . doi: 10.1016/j.cej.2014.09.087

86. Mihai M, Huneault MA, Favis BD (2009) Crystallinity development in cellular poly(lactic acid) in the presence of supercritical carbon dioxide. J Appl Polym Sci 113:2920–2932 . doi: 10.1002/app.30338

87. Zhai W, Ko Y, Zhu W, Wong A, Park C (2009) A Study of the Crystallization, Melting, and Foaming Behaviors of Polylactic Acid in Compressed CO2. Int J Mol Sci 10:5381–5397 . doi: 10.3390/ijms10125381

88. Yu L, Liu H, Xie F, Chen L, Li X (2008) Effect of annealing and orientation on microstructures and mechanical properties of polylactic acid. Polym Eng Sci 48:634–641 . doi:

    10.1002/pen.20970

89.   Tsai CC, Wu RJ, Cheng HY, Li SC, Degradation … S-YY (2010) Crystallinity and dimensional stability of biaxial oriented poly (lactic acid) films. Polym Degrad. doi: 10.1016/j.polymdegradstab.2010.02.032

90.   Houichi H, Maazouz A, Elleuch B (2015) Crystallization behavior and spherulitic morphology of poly(lactic acid) films induced by casting process . Polym Eng Sci 55:1881–1888 . doi: 10.1002/pen.24028

91.   Schmack G, Jehnichen D, Vogel R, Tändler B, Beyreuther R, Jacobsen S, Fritz H-G (2001) Biodegradable fibres spun from poly (lactide) generated by reactive extrusion . J Biotechnol 86: . doi: 10.1016/S0168-1656(00)00410-7

92.   Fambri L, Pegoretti A, Fenner R, Incardona SD, Migliaresi C (1997) Biodegradable fibres of poly (L-lactic acid) produced by melt spinning . Polymer (Guildf) 38: . doi: 10.1016/S0032-3861(96)00486-7

93.   Shim E, Pourdeyhimi B, Shiffler D (2016) Process-structure-property relationship of melt spun poly(lactic acid) fibers produced in the spunbond process . J Appl Polym Sci 133: . doi: 10.1002/app.44225

94.   Hossain KM, Parsons AJ, Rudd CD, Ahmed I, Thielemans W (2014) Mechanical, crystallisation and moisture absorption properties of melt drawn polylactic acid fibres . Elsevier Ltd 53 IS-: . doi: 10.1016/j.eurpolymj.2014.02.001

95.   Northcutt LA, Orski SV, Migler KB, Kotula AP (2018) Effect of processing conditions on crystallization kinetics during materials extrusion additive manufacturing. Polym (United Kingdom) 154:182–187 . doi: 10.1016/j.polymer.2018.09.018

96.   McIlroy C, Graham RS (2018) Modelling flow-enhanced crystallisation during fused filament fabrication of semi-crystalline polymer melts. Addit Manuf 24:323–340 . doi: 10.1016/j.addma.2018.10.018

97.   Tymrak BM, Kreiger M, Pearce JM (2014) Mechanical properties of components fabricated with open-source 3-D printers under realistic environmental conditions. Mater Des 58:242–246 . doi: 10.1016/j.matdes.2014.02.038

98.   Wang L, Gramlich WM, Gardner DJ (2017) Improving the

impact strength of Poly(lactic acid) (PLA) in fused layer modeling (FLM). Polymer (Guildf) 114:242–248 . doi: 10.1016/j.polymer.2017.03.011

99. Chacón JM, Caminero MA, García-Plaza E, Núñez PJ (2017) Additive manufacturing of PLA structures using fused deposition modelling: Effect of process parameters on mechanical properties and their optimal selection. Mater Des 124:143–157 . doi: 10.1016/j.matdes.2017.03.065